15th IFK
Proc. of the 15th International Fluid Power Conference <Symposium/Conference>
<DOI>

New Prototype of High-Speed External Gear Pump Filling Oil from Tooth Root

Rongfu Tang[1,2], Hong Ji[1,2], Bo Lin[3,4], Fei Sun[1,2]

[1]*Key Laboratory of Advanced Pumps, Valves and Fluid Control System of the Ministry of Education, Lanzhou University of Technology, Lanzhou 730050, China;* [2]*College of Energy and Power Engineering, Lanzhou University of Technology, Lanzhou 730050, China;* [3]*Guangxi Liugong Machinery Co., Ltd, Liuzhou 545001, China;* [4]*Guangxi Liugong Yuanxiang Technology Co., Ltd, Liuzhou 545001, China.*

tangrflut@163.com jihong@lut.edu.cn linbo@liugong.com 804216706@qq.com

Abstract.

To overcome the speed limitation of conventional external gear pumps (CEGPs) due to insufficient oil suction efficiency, a novel external gear pump (NEGP) based on tooth root-tooth tip distribution principle is proposed. A comprehensive flow-pressure mathematical model and flow field simulations are developed to analyze the tooth cavity suction process, revealing the key mechanisms responsible for inadequate oil filling in CEGPs. Additionally, the concepts of effective oil suction angle and efficient oil suction angle are introduced to facilitate a comprehensive quantitative analysis. Guided by these findings, an enhanced NEGP configuration integrating a "π"-shaped axial flow groove and a centrifugal flow baffle plate is designed to improve suction capability. This design significantly increases the effective suction area, suppresses centrifugal oil shedding, and enables dual-path oil intake via both tooth root and tooth tip, thereby extending the efficient suction angle. Both simulation and experimental results confirm the superior performance of the proposed NEGP, demonstrating a volumetric efficiency that is 12.1 percentage points higher than that of the CEGP at 3000 rpm.

Keywords. External gear pump, tooth root-tooth tip distribution principle, volumetric efficiency, effective oil suction angle, efficient oil suction angle

1. INTRODUCTION

External gear pumps are widely employed in construction machinery, automotive systems, aerospace, and other industrial applications due to their simple structure, low cost, and strong resistance to contamination. To align with the efficient operating range of electric motors, gear pumps are increasingly designed for higher speeds and miniaturization. However, the maximum rotational speed of conventional high-power external gear pumps (displacement

≥ 60 ml) is typically limited to 2500 rpm. Exceeding this threshold leads to a significant decline in volumetric efficiency, resulting in reduced energy utilization and difficulty in achieving high-speed design objectives.

The volumetric efficiency of hydraulic pumps is primarily influenced by two factors. The first is internal leakage, particularly that occurring at the gear end-face clearance, which accounts for approximately 70% of total leakage [1]. The second factor is suction efficiency, which becomes especially critical under high-speed operating conditions. Suction efficiency is governed by multiple parameters, including tooth number [2], tooth profile [3], size and orientation of the suction port [4,5], pipeline diameter and filter screen porosity [6,7], as well as pump speed [8], suction pressure [9], and the physical and chemical properties of the hydraulic fluid [10].

Various approaches to improving oil suction efficiency have been proposed in the existing literature. El-Hadj [11] suggested increasing the diameter of the suction port to reduce suction resistance. However, Corvaglia's subsequent research revealed that when the inlet diameter exceeds a certain threshold, internal recirculation occurs at the inlet, impeding oil entry into the tooth cavity and reducing its filling capacity [12]. Milani [13] experimentally compared the effects of single versus double suction ports on volumetric efficiency and found that the dual-port configuration significantly enhances pump performance. Bügener [14] applied biomimetic principles to optimize the suction channel structure, thereby improving flow streamline continuity and reducing local flow losses caused by vortices. These studies collectively provide valuable insights for addressing insufficient oil suction in gear pumps under high-speed operating conditions.

This study investigates the phenomenon of inadequate oil suction in CEGP during high-speed operation. A mathematical model of the flow-pressure dynamics during oil suction in the tooth cavity, along with a flow field simulation model, is established to systematically elucidate the underlying mechanisms contributing to reduced suction efficiency. Based on these findings, a novel external gear pump NEGP incorporating a tooth root-tooth tip distribution principle is proposed. Experimental results demonstrate that the NEGP effectively overcomes the speed limitation imposed by poor oil suction efficiency, thereby breaking through a key technical bottleneck. The findings of this research offer a theoretical foundation for the innovative design of high-speed external gear pumps.

2. Analysis of Oil suction Characteristics to CEGP

2.1. CEGP Oil Absorption Efficiency Test

The experimental study focuses on a CEGP with a displacement of V_d=63cm^3/r. The tests were conducted under controlled conditions, with an oil temperature of 44.3°C and an ambient temperature of 27.3°C. The pump operated in an unloaded state to minimize the influence of internal leakage on volumetric efficiency, ensuring that the measured efficiency closely approximates the pump's suction efficiency. The test setup is illustrated in Figure 2.1, where HM46 anti-wear hydraulic oil is used in the reservoir. During testing, the motor drives the CEGP to draw oil from the reservoir through the suction pipe and discharge it back via the discharge pipe, forming a closed-loop circulation system. High-precision pressure sensors (accuracy: ±0.25%) and temperature sensors (accuracy: ±0.1°C) were installed at the pump inlet and outlet, respectively, to monitor oil pressure and temperature.

A turbine flowmeter with an accuracy of ±0.5% was mounted on the discharge line to measure the volumetric flow rate. After the pump reached steady-state operation, data were acquired using a data acquisition system at a sampling frequency of 10 Hz over a 20-second interval, and each test was repeated three times to ensure measurement reliability.

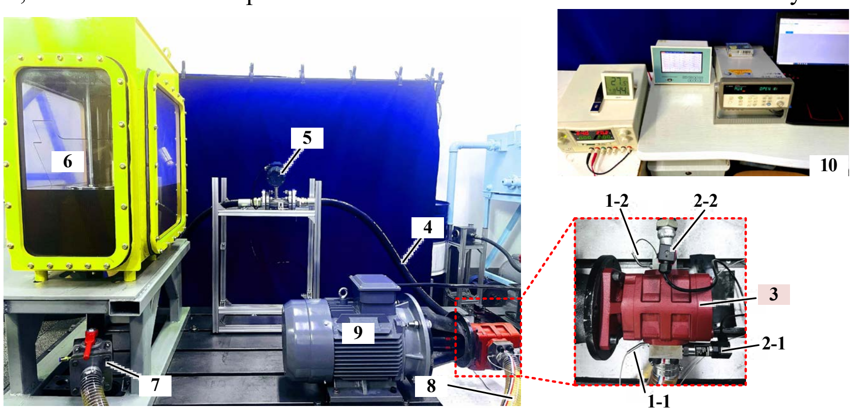

1-Temperature sensor 2-Pressure sensor 3-CEGP 4-Discharge pipe 5-Turbine flowmeter
6-Oil tank 7-Switch valve 8-Suction pipe 9-Motor

Figure 2.1. Experiment System for External Gear Pump

The time-averaged value was computed for each of the three data sets, and the arithmetic mean of these averages was calculated and denoted as Q_C. Subsequently, the volumetric efficiency η_C of the gear pump at various rotational speeds n was determined using Equation (2.1), with results presented in Figure 2.2. As shown by the experimental curve, η_C initially increases and then decreases with rising speed. Specifically, η_C gradually rises from 87.97% at 500 rpm, reaching a maximum of 94.2% at 2700 rpm. Beyond this point, η_C declines rapidly, dropping to 81.87% at 3000 rpm, representing a reduction of 12.33 percentage points from the peak efficiency. This trend clearly indicates a significant deterioration in oil suction performance at high operating speeds for the CEGP.

$$\eta_c = \frac{Q_c}{n \cdot V_d} \qquad (2.1)$$

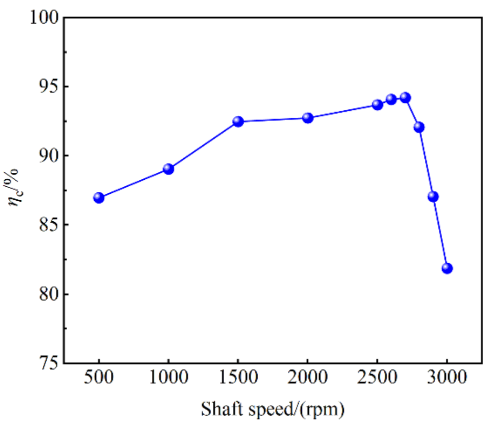

Figure 2.2. Volume efficiency of CEGP at different speeds

2.2. CEGP Cavity Flow - Pressure Characteristics

The CEGP employs a radial oil suction method from the tooth tip. The flow rate entering the tooth cavity is determined by the minimum flow area A formed during gear disengagement. To facilitate analysis, it is assumed that when the gears rotate to a specific angular position, the oil suction process can be approximated as quasi-static. Under this assumption, the minimum pressure difference Δp required for an instantaneous flow rate q to pass through the minimum flow area A is calculated. To clearly differentiate between the two suction configurations, the minimum suction area associated with radial suction from the tooth tip is denoted as A_r, and the corresponding minimum pressure difference is defined as Δp_r. For axial suction from the tooth root, the minimum suction area is denoted as A_a, and the minimum tooth cavity volume is represented as V. The oil flow paths for the two suction methods and the gear structural parameters are illustrated in Figure 2.3.

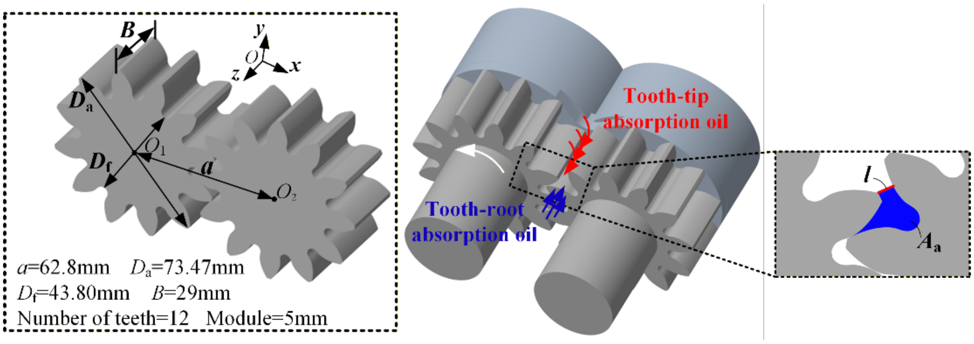

Figure 2.3. Diagram of different oil absorption directions and the gear structural parameters

By integrating 3D model analysis with data fitting, the variations of the shortest inter-tooth distance l, the radial oil suction area A_r, and the axial oil suction area A_a as functions of the rotation angle θ were systematically characterized in a quantitative manner. Consequently, the analytical expressions for A_r, A_a, and the minimum tooth cavity volume V were rigorously derived as follows:

$$l = \begin{cases} 0.063 \ (0° \le \lambda < 14°) \\ 45.83\theta^2 - 14.85\theta + 0.96 \ (14° \le \lambda \le 35°) \end{cases} \quad (2.2)$$

$$A_r = l \cdot B \quad (2.3)$$

$$A_a = 226.84\theta^2 - 1.9\theta + 10.74 \ (0° \le \lambda \le 35°) \quad (2.4)$$

$$V = A_a \cdot B \quad (2.5)$$

$$\begin{cases} \theta = \omega t \\ \lambda = \theta \cdot \dfrac{180}{\pi} \end{cases} \quad (2.6)$$

$$\omega = \frac{2\pi n}{60} \quad (2.7)$$

where ω represents the angular velocity of the gear.

As derived from reference [15], the relationship between flow rate and pressure can be expressed as:

$$q = C_{\rm d} A \sqrt{\frac{2\Delta p}{\rho}} \qquad (2.8)$$

Equation (2.8) can be transformed into

$$\Delta p = \frac{\rho}{2C_{\rm d}^2}\left(B\frac{{\rm d}A_{\rm a}}{{\rm d}t}\right)^2 \frac{1}{A^2} = \delta \cdot \frac{1}{A^2} \qquad (2.9)$$

$$\delta = \frac{\rho}{2C_{\rm d}^2}\left(B\frac{{\rm d}A_{\rm a}}{{\rm d}t}\right)^2 = \frac{\rho}{2C_{\rm d}^2}\left[B\left(453.68\omega^2 t - 1.9\omega\right)\times 10^{-9}\right]^2 \quad (2.10)$$

By substituting equation (2.3) into equation (2.8), the minimum pressure difference $\Delta p_{\rm r}$ required for radial oil suction can be determined. The resulting expression for $\Delta p_{\rm r}$ as a function of angular velocity ω is given by:

$$\Delta p_{\rm r} = \begin{cases} \delta \cdot \dfrac{1}{\left(0.063B\times 10^{-6}\right)^2} & (0° \le \lambda < 14°) \\ \delta \cdot \dfrac{1}{\left[B\left(45.83\omega^2 t^2 - 14.85\omega t + 10.74\right)\times 10^{-6}\right]^2} & (14° \le \lambda \le 35°) \end{cases} \qquad (2.11)$$

Using the discharge coefficient $C_{\rm d} = 0.72$ [1] and fluid density $\rho = 860$ kg/m³, the variation curves of the tooth cavity volume V and the minimum pressure difference $\Delta p_{\rm r}$ with respect to the rotation angle θ are presented in Figure 2.4(a). The detailed profile of $\Delta p_{\rm r}$ within the range of 0 to 0.2 MPa is shown in Figure 2.4(b), where the yellow-shaded region indicates the minimum tooth cavity volume at a rotational speed of 2000 rpm under the condition that $\Delta p_{\rm r} \ge 0.1$ MPa.

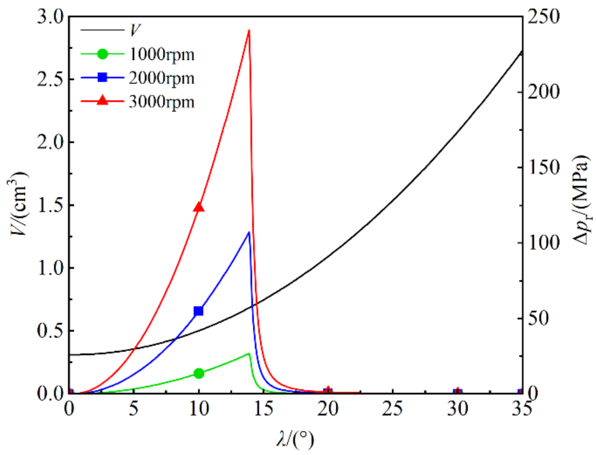

(a)$\Delta p_{\rm r}$ global diagram

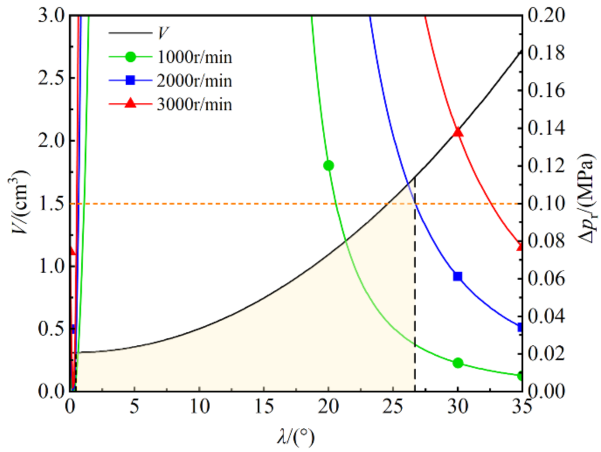

(b) Local graph of Δp_r from 0 to 0.2 MPa

Figure 2.4. V and Δp_r change curves with λ

As illustrated in Figure 2.4, under the tooth tip radial oil suction configuration, at rotational speeds of 1000, 2000, and 3000 rpm, the minimum proportions of the tooth cavity volume satisfying the condition $\Delta p_r \geq 0.1$ MPa account for 29.77%, 52.55%, and 83.07% of the total tooth cavity volume, respectively. This increasing trend demonstrates that higher rotational speeds require a larger angular range over which the gear pump must maintain sufficient oil suction pressure to ensure effective filling. However, the oil suction pressure is solely supplied by atmospheric pressure (approximately 0.1 MPa), which significantly reduces the available time for liquid filling. The underlying cause of this limitation is the inherently small radial oil suction area at the tooth tip, which severely constrains the flow runner capacity and thus impedes efficient oil delivery.

2.3. CEGP Internal Flow Field Characteristics

The theoretical analysis presented in Section 1.2 is confined to the flow–pressure difference relationship during the initial formation stage of the tooth cavity and does not yield an analytical solution for the internal flow dynamics after the cavity is fully developed. To address this limitation, the present study employs Pumplinx software to conduct numerical simulations. The RNG k-ε turbulence model is adopted to accurately capture turbulent flow characteristics. Boundary conditions are defined as follows: the inlet is assigned an absolute pressure of 0.1 MPa, and the outlet is set to 0.3 MPa. The oil properties are specified with a dynamic viscosity of 0.037 Pa·s and a density of 860 kg/m³, while the gear rotational speed is fixed at 2500 rpm. To ensure mesh independence, the outlet flow rate is monitored across different grid resolutions. The resulting simulation data are illustrated in Figure 2.5.

As illustrated in Figure 2.5, the time-averaged volumetric flow rate gradually converges with increasing cell density. When the cell count rises from 8.0×10^5 to 11.3×10^5, the flow rate variation is only 0.28%, which satisfies the criterion for mesh independence. Therefore, considering the balance between computational efficiency and numerical accuracy, a cell size of 8.0×10^5 is selected for all subsequent simulations.

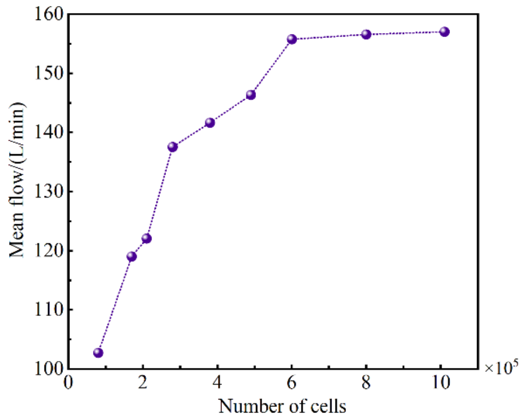

Figure 2.5. The output flow of the CEGP simulation model under different cell numbers

Furthermore, by monitoring the outlet flow rate in the CEGP simulation, the relationship between the volumetric efficiency η_{CS} and rotational speed is established, along with the difference between the simulated value η_{CS} and the experimental value η_C, as depicted in Figure 2.6. As illustrated in Figure 6, the trend of η_{CS} with respect to rotational speed is in good agreement with the experimental results. The maximum and average absolute differences $|\eta_{CS}$-$\eta_C|$ are 2.6% and 1.11%, respectively. The small discrepancy between simulation and test values indicates that the numerical model exhibits high reliability.

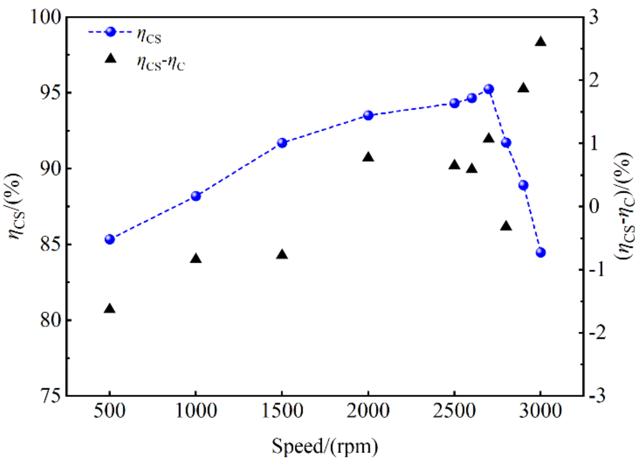

Figure 2.6. η_{CS} and(η_{CS}-η_C) of EGP at different rotational speeds

As shown in Figure 2.7, the streamline distribution within the CEGP at rotational speeds ranging from 2700 to 3000 rpm is presented. With increasing rotational speed, the number of streamlines entering the vortex region gradually increases, and the spatial extent of the vortex expands significantly. Concurrently, the effective flow area into the tooth cavity diminishes, and the density of streamlines decreases accordingly. This vortex structure impedes the normal inflow of oil into the tooth cavity. The underlying mechanism is attributed to the high centrifugal pressure generated within the fully formed tooth cavity due to the rotating gear’s centrifugal force, which intensifies with rotational speed. Under this pressure gradient, part of the oil is expelled radially outward and collides with incoming oil flowing in the opposite direction, thereby inducing localized vortex formation.

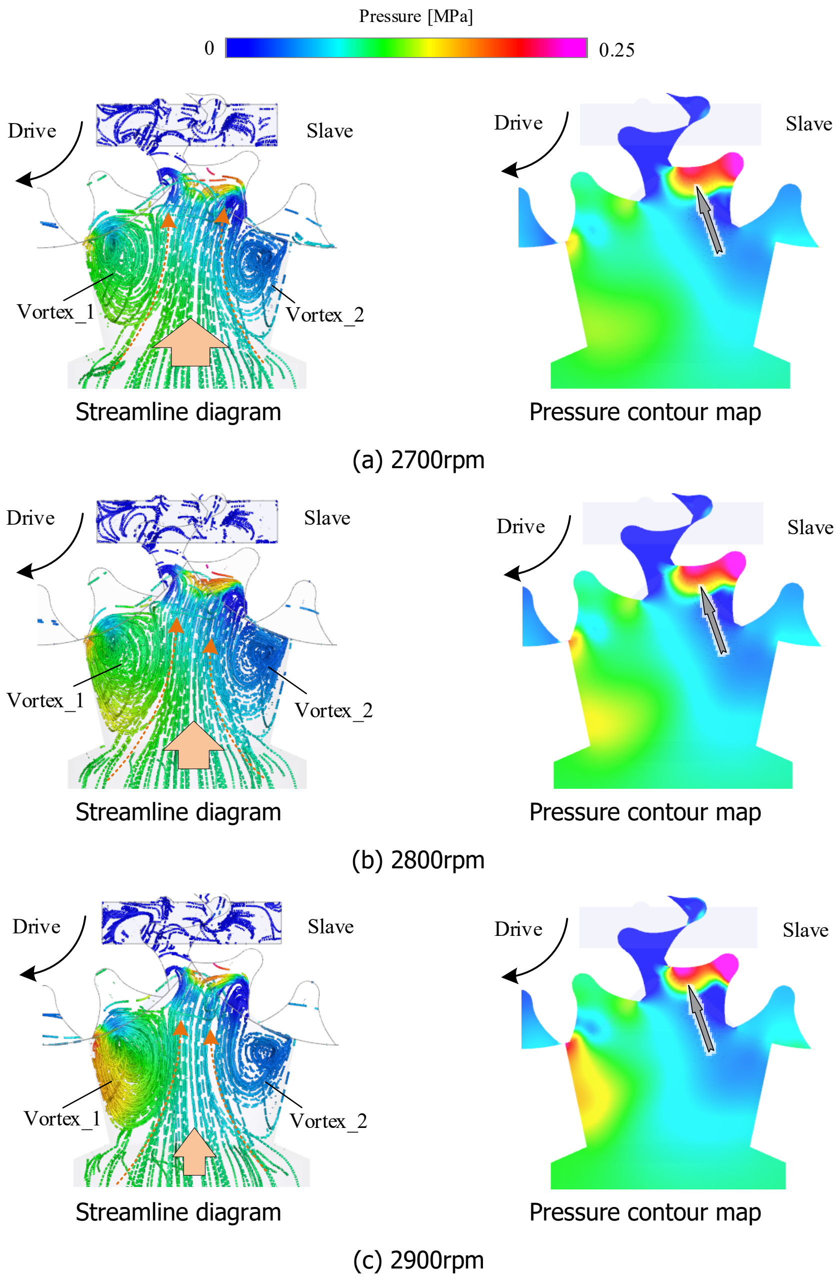

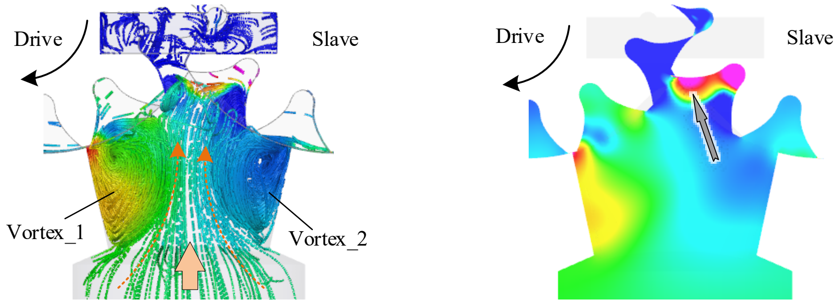

Streamline diagram

Pressure contour map

(d) 3000rpm

Figure 2.7. Inlet flow diagram of CEGP at different speeds

Based on the above analysis, the high-speed oil suction deterioration process in CEGP can be characterized by three progressive stages. First, as the gear teeth begin to disengage and form a complete tooth cavity, the radial oil suction at the tooth tip is insufficient to meet the required flow rate, resulting in a low cavity filling efficiency. Second, under the influence of high rotational speed and centrifugal force, part of the oil within the fully formed cavity is expelled radially outward, further reducing the filling level. Finally, the expelled oil collides with the incoming radial flow, generating two prominent local vortices at the pump inlet that significantly impede the subsequent oil suction process.

2.4. Effective Oil Suction Angle and Efficient Oil Suction Angle

To further analyze the influence of flow characteristics at each stage on the tooth cavity's oil suction efficiency, two key angular parameters are defined: the effective oil suction angle and the efficient oil suction angle. The effective oil suction angle refers to the angular range over which the tooth cavity can freely absorption and discharge fluid, with its filling performance influenced by the radial oil suction area and the inlet vortex. The efficient oil suction angle denotes the portion within the effective oil suction angle where the cavity filling rate is not constrained by these two factors and can achieve an ideal, loss-free filling state.

The geometric definitions of these angles are illustrated in Figure 2.8 and described as follows:

Effective oil suction angle α: This denotes the angular displacement between the line c_1, which connects the edge position of the pump body's oil suction port to the gear center, and the $+x$ reference axis.

Radial oil suction area influence angle β: As introduced in Section 1.3, this represents the angular displacement during which $\Delta p_r \geq 0.1$ MPa, reflecting the extent to which the radial oil suction area limits oil inflow.

Inlet vortex influence angle γ: This is the angle between line c_1 and line c_3, where c_3 is drawn from the gear center tangent to the boundary of the inlet vortex influence zone. It quantifies the angular extent of obstruction caused by the inlet vortex.

Finally, the efficient oil suction angle φ is determined by the equation φ=α-β-γ, representing the optimal angular range for oil suction that remains unaffected by hydraulic losses.

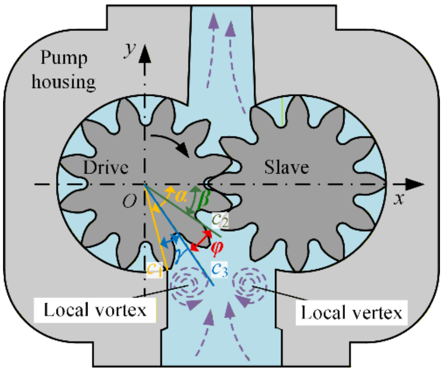

Figure 2.8. Diagram of α, β, γ, φ

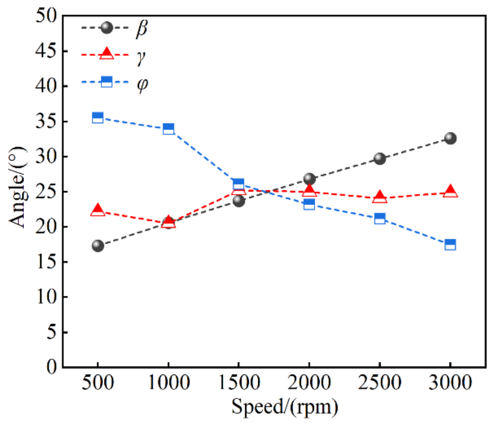

Figure 2.9. The change curve of the β, γ and φ with speed

The variation of each angular parameter with rotational speed is presented in Figure 2.9. As shown in the figure, the radial oil suction area influence angle β increases significantly with rising rotational speed, whereas the inlet vortex influence angle γ exhibits a moderate upward trend with a relatively limited increment. Under these conditions, the efficient oil suction angle φ, primarily governed by the rapid expansion of β, decreases sharply as rotational speed increases, leading to a substantial reduction in the effective liquid filling time of the tooth cavity.

3. Design Principles and Verification for NEGP

Based on the aforementioned analysis, the efficient oil suction angle is primarily constrained by two factors: the radial oil suction area and the inlet-localized vortex. Therefore, the NEGP structural optimization proposed in this study is conducted with respect to these two aspects.

3.1. Design of the New Distribution Structure for NEGP

(1) Centrifugal Flow Baffle Plate and Radial Flow Distribution Groove

According to the analysis in Section 2.3, the local vortex at the inlet is primarily caused by the centrifugal force generated during high-speed gear rotation, which drives the oil out of the tooth cavity. To mitigate this phenomenon, a centrifugal flow baffle plate is incorporated into the pump housing to prevent oil from being expelled under centrifugal force. Additionally, to maintain an adequate low-pressure oil suction passage in the tooth tip region, a radial distribution groove is machined at the center of the flow baffle plate, thereby balancing the dual requirements of flow containment and sufficient oil supply.

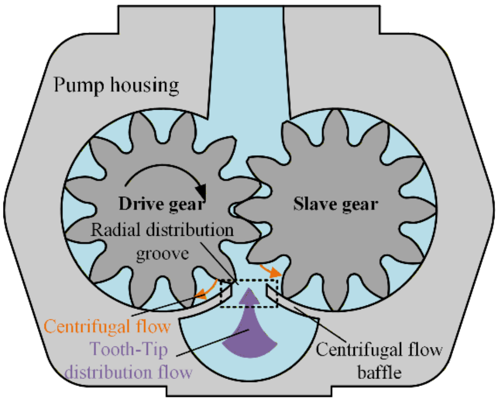

Figure 3.1. Diagram of Tooth-Top distribution flow

(2) "π" -shaped axial flow distribution groove

As described in Section 2.2, single radial oil suction at the tooth tip requires a relatively high suction pressure differential due to its limited flow area, making it prone to becoming a flow bottleneck under high-speed operating conditions. According to Equation (3.1), the centrifugal force acting on a fluid element is directly proportional to the radius of gyration and the square of the rotational speed. Consequently, the centrifugal pressure in the tooth root region is lower than that in the tooth tip region.

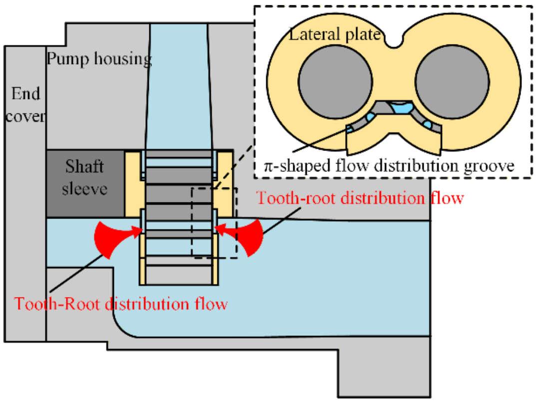

Figure 3.2. Diagram of Tooth-Root distribution flow

To address this imbalance, a π-shaped axial flow distribution groove is machined into the floating lateral plate adjacent to the gear tooth root and connected to the axial suction runner. This feature establishes an auxiliary suction path characterized by lower centrifugal pressure, thereby compensating for insufficient oil supply at the tooth tip by enhancing suction capacity at the tooth root. As this design primarily leverages and enhances the inherent suction potential in the tooth root region, it is termed tooth-root flow distribution. The detailed configuration is illustrated in Figure 3.2.

$$p = \rho\omega^2 \frac{r^2}{2} + p_0 \qquad (3.1)$$

where r is the radial radius.

The radial distribution groove and the π-shaped axial distribution groove collectively constitute the root-to-tip flow distribution system. When flow allocation is based on suction area, the radial suction flow rate $q_{r,c}$ can be calculated using Equation (3.2). Likewise, the volume delivered to the tip tooth cavity $V_{r,c}$ is derived from Equation (3.3).

$$q_{r,c} = q \cdot \frac{A_r}{A_r + 2A_a} \qquad (3.2)$$

$$V_{r,c} = V \cdot \frac{A_r}{A_r + 2A_a} \qquad (3.3)$$

Substituting equation (3.2) into equation (2.9) yields

$$\Delta p_{r,c} = \frac{\rho}{2C_d^2} \cdot {q_{r,c}}^2 \frac{1}{A_r^2} \qquad (3.4)$$

The results calculated from Equations (3.3) and (3.4) are presented in Figure 3.3.

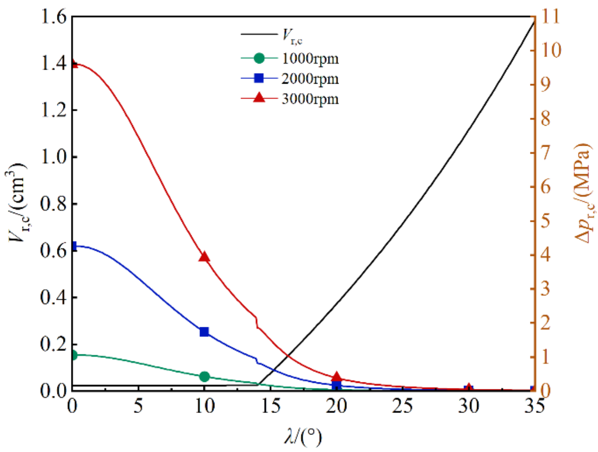

Figure 3.3. $V_{r,c}$ and $\Delta p_{r,c}$ change curves with λ

It can be observed that the pressure difference $\Delta p_{r,c}$ required for parallel oil suction is significantly lower than that of Δp_r under single radial oil suction. At rotational speeds of 1000, 2000, and 3000 rpm, the proportions of the total tooth cavity volume experiencing a pressure difference exceeding 0.1 MPa under the parallel oil suction mode are 4.26%, 22.5%, and 40.45%, respectively, reflecting reductions of 25.51, 30.05, and 42.62 percentage points relative to the single radial oil suction mode. These findings provide theoretical validation that the parallel oil suction configuration at both the tooth root and tooth tip effectively improves oil suction conditions at high rotational speeds and exhibits superior oil suction performance.

3.2. Internal Flow Field Characteristics of NEGP

Under the same simulation conditions as those applied to CEGP, the fluid domain model of NEGP was analyzed. The volumetric efficiency of NEGP at various rotational speeds is presented in Figure 3.4. The results show that the volumetric efficiency increases rapidly with rising rotational speed within the range of 500 to 2500 rpm, while the rate of increase diminishes in the high-speed range from 2600 to 3000 rpm. Compared with the simulation data for CEGP, NEGP exhibits a volumetric efficiency improvement of 2.18%, 5.0%, and 9.61% at 2800, 2900, and 3000 rpm, respectively—demonstrating that the new distribution structure offers significant performance advantages under high-speed operating conditions.

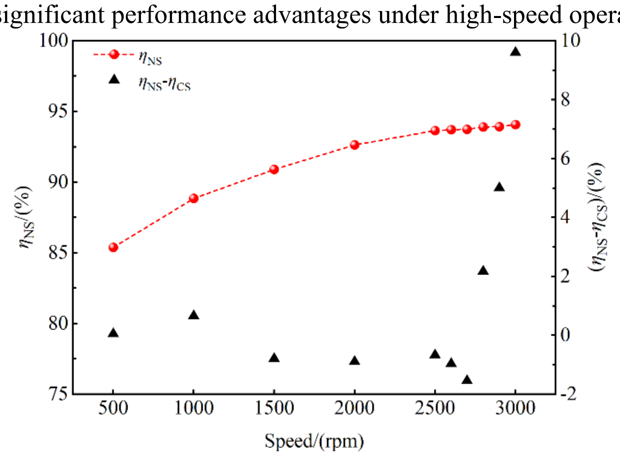

Figure 3.4. Volumetric efficiency of NEGP' simulation model

Figure 3.5 shows the internal streamline distribution of the NEGP at a specific angle under a rotational speed of 3000 rpm. As can be seen from the figure, no local vortices occur in the inlet area, and the oil is clearly divided into three independent and smooth streamlines entering the tooth cavity.

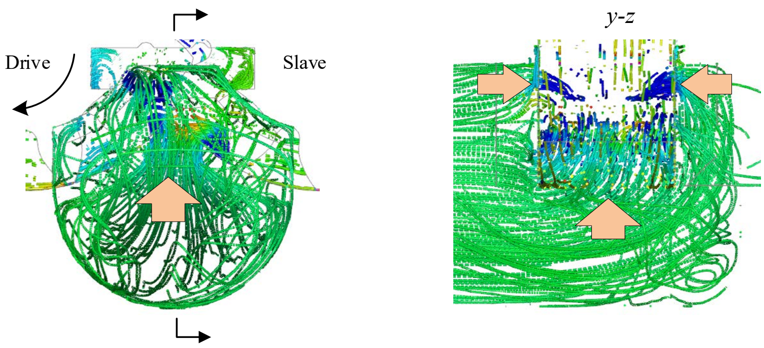

Figure 3.5. Inlet streamline figures of NEGP under 3000rpm

Figure 3.6 further illustrates the variation in angular parameters of NEGP. For NEGP, the vortex influence angle γ remains consistently zero, attributable to the optimized inlet flow field that effectively eliminates local vortices. Although the oil suction area influence angle

β increases rapidly with rotational speed, leading to a reduction in the effective oil suction angle φ, the value of φ at 3000 rpm is increased by 227.54% compared to CEGP. This significant expansion provides substantially improved oil suction duration for the gear pump under high-speed operating conditions, thereby providing a fundamental explanation for its enhanced performance.

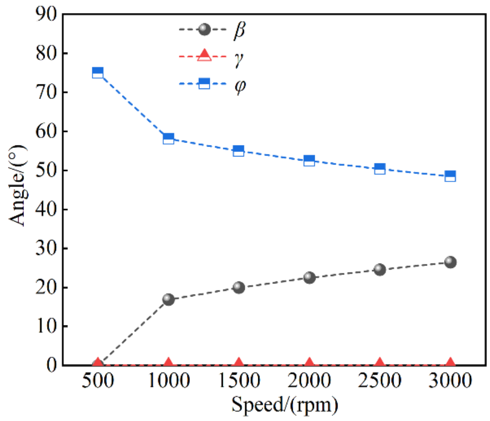

Figure 3.6. The change curve of the β, γ and φ with speed of NEGP

3.3. Experimental Verification to NEGP

To further validate the rationality of the root-to-tip parallel flow distribution principle employed in NEGP, a test bench as shown in Figure 3.7 was constructed, with operating conditions maintained consistently with those of the CEGP test.

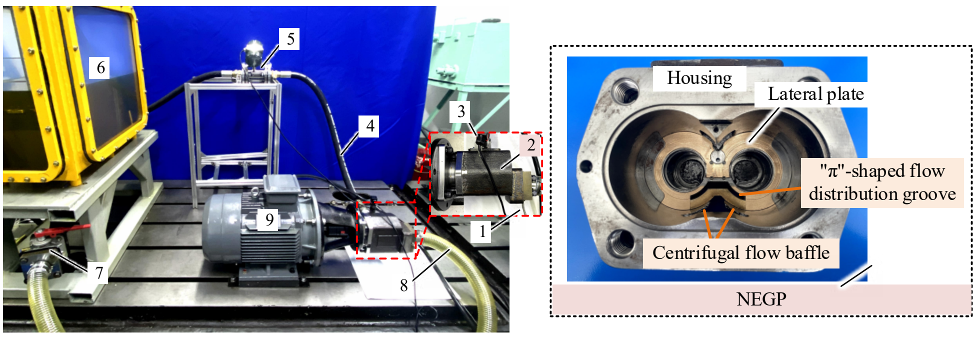

1-Temperature sensor 2- NEGP 3- Pressure sensor 4-Discharge pipe 5-Turbine flowmeter 6-Oil tank 7-Switch valve 8-Suction pipe 9-Motor

Figure 3.7. Experimental bench of NEGP

The volumetric efficiency η_N of the NEGP varies with rotational speed, as shown in Figure 3.8. As can be observed from the figure, the volumetric efficiency of NEGP increases rapidly with rising speed within the range of 500 to 2500 rpm, while the rate of increase slows in the range of 2600 to 3000 rpm, reaching a peak value of 93.97% at 3000 rpm. When the rotational speed exceeds 3000 rpm, η_N begins to decrease, dropping to 79.51% at 4000 rpm. Compared with the efficiency η_C of CEGP, η_N exhibits only a small difference within the 500-2700 rpm range. However, at 2800, 2900, and 3000 rpm, η_N improves by 1.71, 6.92, and 12.1 percentage points, respectively. Based on these results, 2700 rpm can be identified as the critical speed for significant improvement in NEGP's volumetric efficiency. The experimental results clearly demonstrate that NEGP effectively extends the speed range for efficient oil suction and offers distinct performance advantages under high-speed operating conditions.

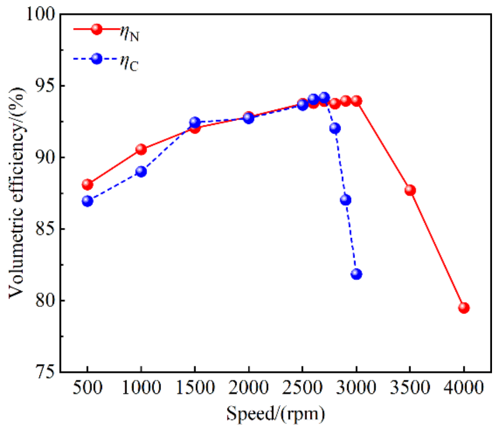

Figure 3.8. Volumetric efficiency of NEGP under different speeds

4. CONCLUSION

The intrinsic mechanism underlying the decline in oil suction efficiency of CEGP under high-speed operation was el1ucidated. This process can be divided into three stages: First, during the initial cavity formation stage, the narrow radial oil suction area at the tooth tip results in insufficient initial filling rate. Second, the centrifugal effect induced by high-speed rotation expels oil from the cavity, further reducing the filling rate. Third, the expelled oil collides with radially incoming oil at the pump inlet, generating two large local vortices that impede radial oil suction at the tooth tip. Collectively, these factors lead to a significant reduction in the effective oil suction angle of CEGP, inadequate effective filling duration, and ultimately result in poor high-speed oil suction performance and low volumetric efficiency.

A novel external gear pump based on the tooth root-tooth tip parallel distribution principle was proposed. Its innovative design incorporates a π-shaped axial distribution groove on the floating side plate to enhance oil suction capacity in the tooth root region. Additionally, a centrifugal flow baffle plate featuring radial distribution grooves is integrated into the pump housing to suppress centrifugal oil ejection while preserving volumetric oil suction at the tooth tip. The axial and radial distribution grooves serve as the primary pathways for centrifugal oil suction at the tooth root and volumetric oil suction at the tooth tip, respectively, forming a dual-channel oil supply system in NEGP.

Simulation and experimental results validate the superior performance of NEGP. Flow field analysis reveals the absence of local vortices at the NEGP inlet, with the effective oil suction angle being significantly larger than that of CEGP. Experimental data show that the volumetric efficiency of NEGP reaches a peak of 93.97% at 3000 rpm, and its efficient operating range is extended. Comparative performance analysis indicates that, with 2700 rpm identified as the critical speed, the volumetric efficiency of NEGP at 2800, 2900, and 3000 rpm exceeds that of CEGP by 1.71, 6.92, and 12.1 percentage points, respectively.

5. REFERENCES

[1] J. Lin, C. He, ‘Hydraulic Components’, Beijing: Machinery Industry Press, 1988.

[2] V. Ivanov, D. Karaivanov, S. Ivanova, et al., ‘Gear mesh geometry effect on performance improvement for external gear pumps’, MATEC Web Conf., EDP Sciences, 2019. https://doi.org/10.1051/matecconf/201928701007

[3] X. Zhao, A.Vacca, ‘Analysis of continuous-contact helical gear pumps through numerical modeling and experimental validation’, Mech. Syst. Signal. Pr., pp. 352-378, 2018. https://doi.org/10.1016/j.ymssp.2018.02.043

[4] G. Yang, W. Wang, F.Huang, et al., ‘Cavitation characteristics of gear pump under different suction port sizes and speeds’, Chin. Hydraul. Pneum., (01): 74-79, 2020. https://doi.org/10.11832 /j.issn.1000-4858.2020.01.012

[5] Bügener N, Klecker J, Weber J. Analysis and improvement of the suction performance of axial piston pumps in swash plate design[J]. Int. J. Fluid Power., 15(3): 153–167, 2014. https://doi.org/10.1080/14399776.2014.968436

[6] M. Suresh Kumar, K. Manonmani, ‘Computational fluid dynamics integrated development of gerotor pump inlet components for engine lubrication’ Proc. Inst. Mech. Eng., Part D: J. Automob. Eng., 224(12): 1555-1567, 2010. https://doi.org/10.1243/09544070JAUTO1594

[7] M. Suresh Kumar, K. Manonmani, ‘Numerical and experimental investigation of lubricating oil flow in a gerotor pump’, Int. J. Auto. Tech-Kor., 12(6): 903-911, 2011. https://doi.org/10.1007/s12239-011-0103-z

[8] D. del Campo Sud, ‘Analysis of the suction chamber of external gear pumps and their influence on cavitation and volumetric efficiency’, Univ. Politéc. Catal., Dep. Mec. Fluid., 2012.

[9] Y. Zhang, Z. Chen, J. Liao, ‘Effects of pump parameters on the oil absorption characteristics of bidirectional involute internal gear pumps’, Res. Eng., 20: 101405, 2023. https://doi.org/10.1016/j.rineng.2023.101405

[10] B. Wieczorek, Ł. Warguła, O. Zharkevich, et al., ‘The study of the impact of oil type and throttling pressure on the vibrations of a gear pump’, Adv. Sci. Technol. Res. J., 19(5), 142–155, 2025. https://doi.org/10.12913/22998624/201216

[11] A. A. El-Hadj, S. Z. B. Abd Rahim, ‘Optimization of an external gear pump using response surface method’, J. Mech., 36:567-575, 2020. https://doi.org/10.1017/jmech.2020.7

[12] A. Corvaglia, M. Rundo, S. Bonati, et al., ‘Simulation and experimental activity for the evaluation of the filling capability in external gear pumps’, Fluids, 8(9): 251, 2023. https://doi.org/10.3390/fluids8090251

[13] M. Milani, L. Montorsi, F. Paltrinieri, ‘Experimental investigation of the suction capabilities of an innovative high speed external gear pump for electro-hydraulic actuated automotive transmissions’, Int. J. Fluid Power., pp. 243-272, 2024. https://doi.org/10.13052/ijfp1439-9776.2527

[14] N. Bügener, J. Klecker, J. Weber, ‘Analysis and improvement of the suction performance of axial piston pumps in swash plate design’, Int. J. Fluid Power., 15(3): 153-167, 2014. https://doi.org/10.1080/14399776.2014.968436

[15] A. Vacca, G. Franzoni, ‘Hydraulic fluid power: fundamentals, applications, and circuit design’ Hoboken: John Wiley & Sons, 2021.

Biographies

Rongfu Tang received the bachelor's degree in mechatronic engineering from Lanzhou University of Technology in 2019 and has been pursuing a Ph.D. in the same discipline since 2020. His primary research focuses on fundamental studies and applications of modern hydraulic components.

Hong Ji received a Bachelor of Engineering degree in Fluid Transmission and Control from Gansu University of Technology in June 1993, and subsequently earned a Doctor of Engineering degree from Zhejiang University in March 2005. He is currently a Professor and Doctoral Supervisor at the School of Energy and Power Engineering, Lanzhou University of Technology. His primary research focuses on fundamental studies and applications of modern hydraulic components, as well as hydraulic technology for construction machinery.

Bo Lin obtained Ph.D. in Analytical Chemistry from Wuhan University and is currently serving as a Senior Engineer at Guangxi Liugong Machinery Co., Ltd. Her primary research focuses include the development of lubricating materials for construction machinery, the application of non-metallic materials, and advancing material technologies for performance under extreme operating conditions.

Fei Sun received his Doctor of Engineering degree in Mechatronic Engineering from Lanzhou University of Technology in 2024. He is currently serving as a Lecturer in the School of Mechanical and Electrical Engineering at Lanzhou University of Technology, where his research primarily focuses on the integrated design of electro-hydraulic power systems.